Gondwana Research 59 (2018) 76–86

Contents lists available at ScienceDirect

Gondwana Research

journal homepage: www.elsevier.com/locate/gr

A window into the lower crust: Trace element systematics and the occurrence of inclusions/intergrowths in granulite-facies rutile

Emma Hart [a,*], Craig Storey [a], Simon L. Harley [b], Mike Fowler [a]

[a] School of Earth and Environmental Sciences, University of Portsmouth, Portsmouth, UK
[b] School of GeoSciences, University of Edinburgh, Edinburgh, UK

ARTICLE INFO

Article history:
Received 11 September 2017
Received in revised form 14 February 2018
Accepted 27 February 2018
Available online 02 April 2018

Handling Editor: T. Tsunogae

Keywords:
Rutile
UHT granulite
Trace elements
Zr-in-rutile thermometry
Inclusion/intergrowth

ABSTRACT

Rutile occurs as an accessory mineral in many high-temperature metamorphic assemblages and has the potential to identify and investigate UHT metamorphic terranes. Whilst the use of Zr-in-rutile geothermometry to identify ultrahigh-temperature terranes is appealing, its application to granulites can be difficult owing to diffusional resetting of Zr concentrations during cooling and decompression. In order to provide constraints on *P-T* conditions and trace element systematics during ultrahigh-temperature metamorphism, metamorphic rutile in granulites from the Archean Napier Complex and the Palaeozoic Rauer Group, Antarctica have been investigated for trace element composition and mineral inclusions/intergrowths. Textural observations and Zr-in-rutile temperatures show that unlike the large proportion of rutiles grains in the matrix, rutile grains that are shielded by phases with low Zr-diffusivities (e.g. orthopyroxene) and/or are in chemical isolation from zircon, have the potential to retain Zr concentrations that correspond to ultrahigh-temperatures. Principal Component Analysis reveals that V, Cr, Nb, Mo, Ta and W are significantly enriched in rutile from Archean and Proterozoic ultrahigh-temperature terranes. High concentrations of elements such as Cr and V indicate a spinel-rich source, demonstrating the effect of protolith bulk chemical composition on rutile trace element signatures. Rutile is shown to contain inclusions and intergrowths of aluminium silicate, quartz, corundum and feldspar, including the first reported occurrence of prograde kyanite, which provides direct evidence that the Napier Complex experienced a typical clockwise *P-T* evolution.

1. Introduction

Ultrahigh-temperature (UHT) metamorphism, a subdivision of granulite facies metamorphism, is defined as crustal metamorphism at temperatures in excess of 900 °C (Harley, 1998a) and at pressures not exceeding the stability field of sillimanite (Kelsey and Hand, 2015; Pauly et al., 2016). UHT metamorphism typically occurs at depths of 20–40 km and on a regional scale provides evidence that major tectonic processes involved in collisional orogenesis may operate under extreme thermal conditions (Harley, 2008). In order to provide key constraints on tectonothermal models, it is important to obtain accurate *P-T* records for UHT terranes. However, the ability to identify UHT terranes is potentially hampered as the application of conventional element exchange geothermometry to granulites is notoriously difficult owing to diffusional resetting during cooling (Pape et al., 2016).

Rutile geochemistry is widely used to reconstruct *P-T* histories of metamorphic terranes, as it is a common accessory mineral in many metamorphic assemblages and is stable over a large *P-T* range. It is resistant to retrogression and fluid infiltration and can therefore give an insight to the metamorphic history of a rock even when evidence of metamorphism has been partially obliterated in the matrix. The robust nature of rutile during diagenetic processes also makes it a useful tool in sedimentary provenance studies as it retains geochemical information from the source rock. It has a strong affinity for high field strength elements, such as Nb, Ta and Cr, which can be used to constrain geological processes (e.g. subduction zone metamorphism) and deduce source rock lithology (Zack et al., 2004b; Triebold et al., 2007). Metamorphic temperatures of rutile growth can also be obtained using the Zr-in-rutile geothermometer as the partitioning of Zr into rutile has proven to be strongly temperature dependent in rocks where rutile is in coexistence with zircon and quartz (e.g. Zack et al., 2004a; Watson et al., 2006; Tomkins et al., 2007). Furthermore, it has recently been demonstrated that metamorphic rutile can preserve mineral inclusions of prograde and peak metamorphic phases (Hart et al., 2016).

Whilst Zr-in-rutile thermometry is a powerful tool when investigating metamorphic terranes, the application of the thermometer to rutile from UHT terranes often returns lower temperatures than expected. Although the Zr-in-rutile geothermometer can record ultrahigh-temperatures (>900 °C), Zr concentrations within granulite-facies rutile are often variably reset during cooling and decompression making Zr-in-rutile temperature data difficult to interpret. Recent studies have

* Corresponding author.
E-mail address: emma.hart@port.ac.uk. (E. Hart).

https://doi.org/10.1016/j.gr.2018.02.021

shown that whilst Zr concentrations are often homogenous within individual rutile grains, concentrations can vary up to several thousand μg/g on the thin-section scale (e.g. Zack et al., 2004a; Luvizotto and Zack, 2009; Jiao et al., 2011; Meyer et al., 2011; Kooijman et al., 2012; Ewing et al., 2013; Taylor-Jones and Powell, 2015; Kelsey and Hand, 2015; Harley, 2016). Rutile grains that exhibit the lowest Zr concentrations are reported to occur either in close proximity to Zr-bearing phases or contain zircon/baddeleyite exsolution lamellae. Furthermore, the application of trace element discrimination, such as the Nb/Cr discrimination diagram which is used to differentiate between metapelitic and metamafic source rock lithologies (Zack et al., 2004b; Triebold et al., 2007; Meinhold et al., 2008), often produces unsystematic results with granulite-facies rutile being misleadingly classified (Meyer et al., 2011; Kooijman et al., 2012).

To resolve these issues and further utilise rutile as a tool to identify and investigate UHT terranes, trace element concentrations have been analysed in metamorphic rutile from the granulite-facies paragneisses of the Napier Complex and the Rauer Group, Antarctica. Trace elements which may be useful for identifying rutile from UHT terranes have been characterized by comparing rutile trace element chemistry in Archean and Proterozoic UHT rocks to younger HP-LT metapelitic and metamafic rocks. The reliability of the Zr-in-rutile thermometer has also been investigated by analysing the Zr concentrations of rutile found within the matrix and as inclusions within other phases, and evaluating the link between Zr concentrations and the textural setting of rutile in relation to Zr-bearing phases. Mineral inclusions and intergrowths in rutile have been sought to aid the interpretation of Zr-in-rutile temperature data and to place important constraints on the conditions of prograde metamorphism.

2. Geological settings

2.1. Napier Complex

The Napier Complex of Enderby Land, East Antarctica, is a late Archean high-grade terrane which consists predominantly of tonalitic and granitic orthogneiss (charnockite and enderbite) with layered metasediments and minor mafic/ultramafic granulites (Sheraton et al., 1987; Harley and Black, 1997; Hokada et al., 2003). As well as comprising some of the oldest rocks on Earth (*c.* 3.8 Ga; Harley and Black, 1997), the Napier Complex also preserves evidence of UHT metamorphism that occurred at temperatures in excess of 1000 °C. The Amundsen Bay area in the western part of the Complex (Fig. 1a) is thought to have experienced the highest-grade metamorphism based on the occurrence of sapphirine + quartz and osumilite assemblages (e.g. Dallwitz, 1968; Sheraton et al., 1987; Harley and Henson, 1990; Harley and Motoyoshi, 2000; Tsunogae et al., 2002; Hokada et al., 2008; and references therein).

Based upon geochronological data, it has been proposed that UHT granulite-facies metamorphism took place during the Neoarchean and Early Paleoproterozoic (*c.* 2.5 Ga; Harley and Black, 1997; Carson et al., 2002; Hokada et al., 2003, 2004, 2008; Kelly and Harley, 2005; Horie et al., 2012; Harley, 2016). Peak *P-T* conditions of >1170 °C and 6–11 kbar have been proposed on the basis of mineral assemblage stability (sapphirine + quartz) and conventional geothermometry (e.g. Harley and Motoyoshi, 2000; Tsunogae et al., 2002; Shimizu et al., 2013). Petrological studies also show that following peak metamorphic conditions, the complex followed a near-isobaric cooling trajectory down to 650 °C and 7 kbar (e.g. Harley, 2016).

2.2. Rauer Group

The Rauer Group is a granulite-facies terrane on the Prydz Bay coast, East Antarctica (Fig. 1b), consisting of reworked Mesoproterozoic and Archean rocks which have undergone UHT tectono-metamorphism (Harley, 1998b; Kelsey et al., 2003a, 2007; Tong and Wilson, 2006). In situ (Th + U) − Pb monazite chemical age data for granulite-facies metapelites suggests that the Rauer Group is polymetamorphic (Kelsey et al., 2003a), with tectonothermal events occurring in both the Neoproterozoic (*c.* 1000 Ma) and the early Palaeozoic (*c.* 530 Ma) (Harley, 1998b; Kelsey et al., 2003a, 2007; Tong and Wilson, 2006). It is thought that the Neoproterozoic event is due to late Mesoproterozoic collision and arc accretion (Tong and Wilson, 2006), whereas the early Palaeozoic event is a result of Pan-African orogenesis with the Rauer Group forming part of the Prydz Bay suture related to the amalgamation of east Gondwana (Kelsey et al., 2003b).

The Rauer Group comprises two distinct types of paragneiss which outcrop as discontinuous layers hosted within felsic orthogneiss. The Mather Paragneiss, which outcrops discontinuously along a 3 km strike in the eastern Rauer Group (Mather Peninsula, Short Point and Sticks Island), comprises a variety of Mg–Al-rich lithologies that preserve evidence of late Neoproterozoic to early Palaeozoic UHT metamorphism (Kelsey et al., 2008; Hokada et al., 2016). Rock types which constitute the Mather Paragneiss include Gt-Opx-Sill-Spr migmatite, Opx-Sill quartzite, Gt-bearing quartzite, Gt-bearing mafic granulite, Opx-bearing leucogneiss and forsterite marble (Harley, 1998b), which

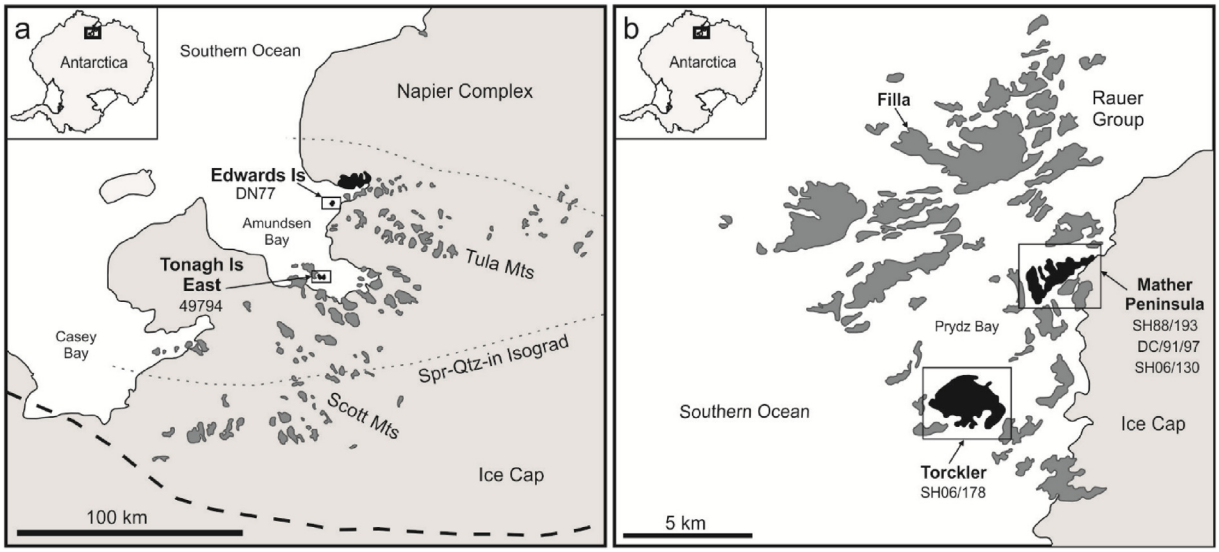

Fig. 1. Simplified geological maps of: (a) Napier Complex, (modified after Carson et al., 2002); (b) Rauer Group (after Tong and Wilson, 2006).

occur as metre-sized boudins hosted by felsic orthogneiss (Harley, 1998b; Kelsey et al., 2003a). Peak metamorphic conditions of 950–1050 °C and 9–12 kbar have been determined based on the occurrence of orthopyroxene-sillimanite-quartz and sapphirine-bearing assemblages, which are indicative of UHT conditions (Harley and Fitzsimons, 1991; Harley, 1998b; Kelsey et al., 2003b).

The Filla Paragneiss on the other hand, which outcrops on most islands and peninsulas throughout the Rauer Group (including Mather Peninsula and Torckler Island), comprises Mesoproterozoic Fe-rich metapelites which host calc-silicate boudins (Harley and Fitzsimons, 1991; Harley and Buick, 1992; Kelsey et al., 2008). Minimum peak metamorphic conditions of 840–960 °C and 7–10 kbar have been proposed for the Filla Paragneiss based on textures and phase relations in wollastonite-scapolite calcsilicates (Harley and Buick, 1992; their Fig. 9). Despite the differences in lithology and *P-T* estimates, recent geochronological studies suggest that the two units have a shared metamorphic history, recording the early Palaeozoic UHT metamorphic event with near-isothermal decompression (Kelsey et al., 2003b, 2007; Hokada et al., 2016).

3. Analytical techniques

Rutiles were prepared for analysis within polished thick sections (*c.* 100 μm). Each section was imaged to identify rutiles, especially those with inclusions. All BSE images were collected using a Zeiss EVO series MA10 scanning electron microscope (SEM) at the University of Portsmouth, with qualitative mineral chemical analysis performed using an Oxford Instruments X-Max EDS (energy dispersive spectrometer) under standard operating conditions of 15 kV accelerating voltage, 3 nA current and at 11–15 mm working distance.

Trace elements in rutile (spot analyses) were determined using an Agilent 7500cs (quadrupole) ICP-MS and an ASI RESOlution excimer laser ablation system at the University of Portsmouth. Rutile was ablated using a 40 μm diameter laser beam at a fluence of 4.50 J/cm^2 and at a repetition rate of 10 Hz. Each analysis consisted of 30 s background and 60 s of sample acquisition. Sixteen trace elements were analysed: ^{45}Sc, ^{51}V, ^{52}Cr, ^{66}Zn, ^{69}Ga, ^{88}Sr, ^{90}Zr, ^{93}Nb, ^{95}Mo, ^{118}Sn, ^{121}Sb, ^{177}Hf, ^{181}Ta, ^{182}W, ^{208}Pb, ^{238}U. Each analytical run consisted of twelve spot analyses bracketed between two analyses of NIST 610 reference material (Pearce et al., 1997), along with four analyses of the secondary rutile reference material R10 (Luvizotto et al., 2009). The NIST 610 reference material was analysed using a 55 μm diameter laser beam, with a 30 μm beam used for the R10 reference material. Measured trace element concentrations for R10 were reproducible and within the uncertainty quoted for the reference values (see Supplementary Material 1). The SILLS software package (Guillong et al., 2008) was used for data reduction, using NIST 610 as the external standard, and by assuming TiO_2 = 98% for internal reference normalization. During data reduction, care was taken to exclude any anomalous analysis due to zircon involvement (i.e. as inclusions or exsolution lamellae).

Matrix minerals and inclusions/intergrowths in rutile were analysed quantitatively for mineral chemistry, using a Cameca SX100 electron microprobe equipped with 5 wavelength dispersive spectrometers and 1 energy dispersive spectrometer at the University of Bristol, with operating conditions of 15–20 kV acceleration voltage and a beam current of 10–20 nA focussed to a 1 μm electron beam. Nine oxides were used to chemically characterize matrix minerals (SiO_2, TiO_2, Al_2O_3, FeO, MnO, MgO, CaO, Na_2O, K_2O). Standards used to calibrate EPMA analysis were: Amelia albite (Na, Si), St Johns olivine (Mg), Eifel sanidine (Al, K), wollastonite (Ca), ilmenite (Ti, Fe) and Mn.

The nature of Al_2SiO_5 polymorphs were determined using Raman spectroscopy, with spectra obtained using a Horiba Jobin Yvon Raman microscope fitted with frequency-doubled Nd:YAG (532 nm) and HeNe (633 nm) lasers at the University of Greenwich. Rayleigh scattering was rejected using long-pass filters and Raman scattering detected using a charge-coupled device. A slit of 100 μm and pinhole of 200 μm were used to minimize contributions from the rutile grain appearing in the spectra of the inclusions/intergrowths. Calibration of the instrument was determined by checking the position of the Si peak at 520.6 cm^{-1}. Spectra were obtained using the 532 nm laser which was focused either down a ×50 or ×100 objective and were captured and processed using Labspec 6 software. Phases were identified with the assistance of the CrystalSleuth software (Laetsch and Downs, 2006). In instances where the mixing of two spectra occurred due to rutile fluorescence, phases were manually checked against published Raman spectra from the RRUFF Project database (Lafuente et al., 2015).

4. Sample descriptions

4.1. Napier Complex

Samples DN77 (Edwards Island) and 49794 (Tonagh Island East) are both medium to coarse grained feldspar granofels. Sample DN77 predominantly comprises plagioclase (andesine) and quartz, with orthopyroxene and sapphirine throughout the matrix (Fig. 2a). Apart from cordierite, which occurs as reaction coronas surrounding sapphirine, the Spr-Opx-Qtz assemblage has been preserved with little evidence of further retrogression. Large rutile grains >350 μm in size, occur at grain boundaries between quartz, feldspar, orthopyroxene and sapphirine and as inclusions within orthopyroxene and quartz. Zircons >50 μm in size are found as inclusions in sapphirine, orthopyroxene and quartz. In sample 49794 the groundmass comprises quartz, K-feldspar, plagioclase (oligoclase) and sillimanite with lenses of sapphirine and orthopyroxene and accessory rutile and zircon (Fig. 2b). Rutile (>100 μm in size) occurs at grain boundaries and as inclusions in quartz and orthopyroxene. Grains of zircon (<30 μm) are found clustered as inclusions in quartz and orthopyroxene.

4.2. Rauer Group

The two samples of Mather Paragneiss, SH88/193 (**L17** 68°51′0″S 77°54′40″E) and DC/91/97 (**L10** 68°51′0″S 77°55′0″E), sampled on the Mather Peninsula are medium to coarse grained metapelites comprising garnet, orthopyroxene, quartz, perthitic feldspar, biotite, sillimanite and accessory rutile and zircon (Fig. 2c–d). SH88/193 additionally contains late phlogopite. Poikiloblastic garnets >1 cm in size contain inclusions of sillimanite, quartz, orthopyroxene and rutile. Rutile occurs at grain boundaries as elongate idioblasts >600 μm in size and as >100 μm inclusions within garnet and quartz. Zircon is found as small 10–150 μm inclusions within garnet and quartz.

Garnet-sillimanite gneisses which form part of the Filla Paragneiss were sampled on the Mather Peninsula and Torckler Island. SH06/178 (T07-7 68°53′2.86″S 77°51′1.65″E), sampled on Torckler Island, is a garnet-sillimanite migmatitic paragneiss with a medium- to coarse-grained groundmass comprising sillimanite, K-feldspar, quartz, biotite, rutile and zircon (Fig. 2e). Sillimanite pseudomorphs after coarse, random, kyanite blasts, can be identified by clusters (>2.5 mm in size) of small high relief crystals with low order grey to yellow birefringence in cross-polarized light (former kyanite proven by electron backscattered diffraction on the pseudomorphs in another sample from Hookah Island).

Sample SH07/130 (M07–3 68°50′9.82″S 77°54′6.36″E) from the west side of the Fillas outcrop on the Mather Peninsula, is a medium- to coarse-grained garnet-sillimanite gneiss with a steep (intense) sillimanite fabric comprising a groundmass of K-feldspar, plagioclase (andesine), quartz, rutile, apatite and zircon (Fig. 2f). In both samples, garnet porphyroblasts >3 mm in size contain inclusions of quartz, sillimanite and rutile. Rutile occurs at grain boundaries as 100–500 μm idioblastic grains, with both rutile and zircon found as 50–100 μm inclusions within quartz, orthopyroxene and garnet.

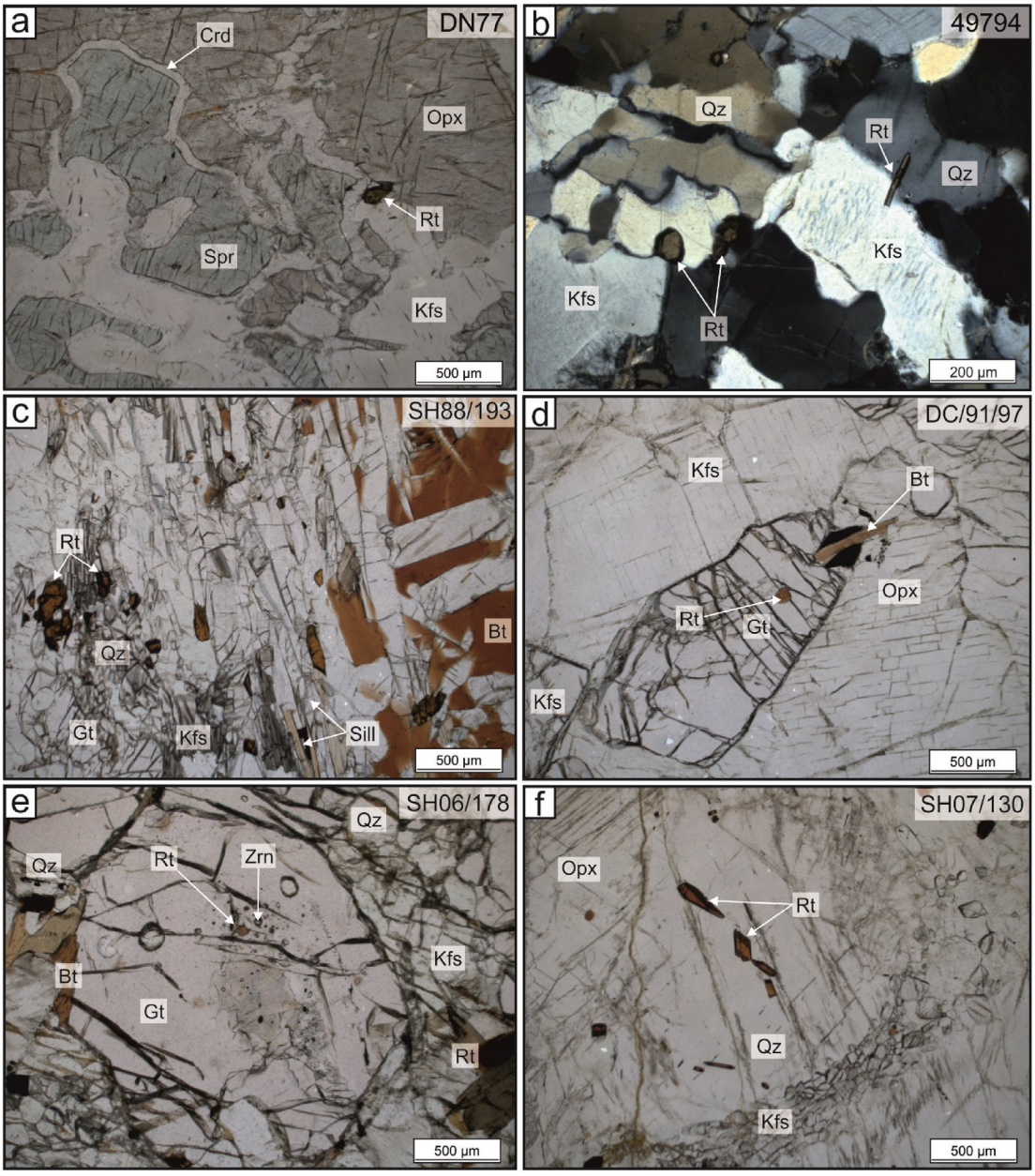

Fig. 2. Photomicrographs of UHT granulites from the Napier Complex (a–b) and the Mather (c–d) and Filla Paragneisses (e–f) from the Rauer Group.

5. Trace element concentrations in rutile

5.1. Principal Component Analysis of trace element concentrations

Whilst bivariate plots can be used to visualize selected differences in rutile trace element chemistry between each of the studied samples, a more comprehensive and unbiased approach is to use multivariate statistics. Principal Component Analysis (PCA) is a multivariate statistical procedure which takes all the variables in a dataset (in this case trace elements) and aims to identify those which explain the most variance between samples on a single diagram (Fig. 3). The first principal component (PC1) explains most of the variance within a dataset, followed by the second principal component (PC2) which explains the second greatest variance orthogonal to the first.

In this study, PCA has been applied to trace element concentrations in rutile using eight variables (Sc, V, Cr, Zn, Nb, Mo, Ta, W). Zr and Hf concentrations were excluded from PCA as they are temperature-dependent and often reset as a result of post-peak processes. Trace element concentrations at or below detection limits have been excluded to avoid significant bias (for full trace element concentrations see Supplementary Material 2), and a logarithmic transformation (Log10) was applied to the dataset to ensure that all data is on the same scale to avoid anomalous outliers. PCA was conducted using Minitab® 18 Statistical Software.

The PCA plots in Fig. 3 are a combination of loadings and scores. "Loadings" refer to the distribution of the variables with respect to PC1 and PC2, and "scores" refer to the distribution of samples. Fig. 3a shows a distinct difference in rutile trace element chemistry between the studied samples with the Napier Complex rutiles positively loaded onto PC1 (plotting on the right of the diagram) and rutiles from the Mather and Filla paragneisses (Rauer Group) negatively loaded onto PC1 (plotting on the left). Rutiles from the two Napier Complex samples have a similar trace element signature characterized by high concentrations of Nb, Mo, Ta and W and lower concentrations of V and Cr (Fig. 3a). Mo and W concentrations are remarkably high in the Napier Complex rutiles with 5–600 ppm Mo and 190–1240 ppm W (Supplementary

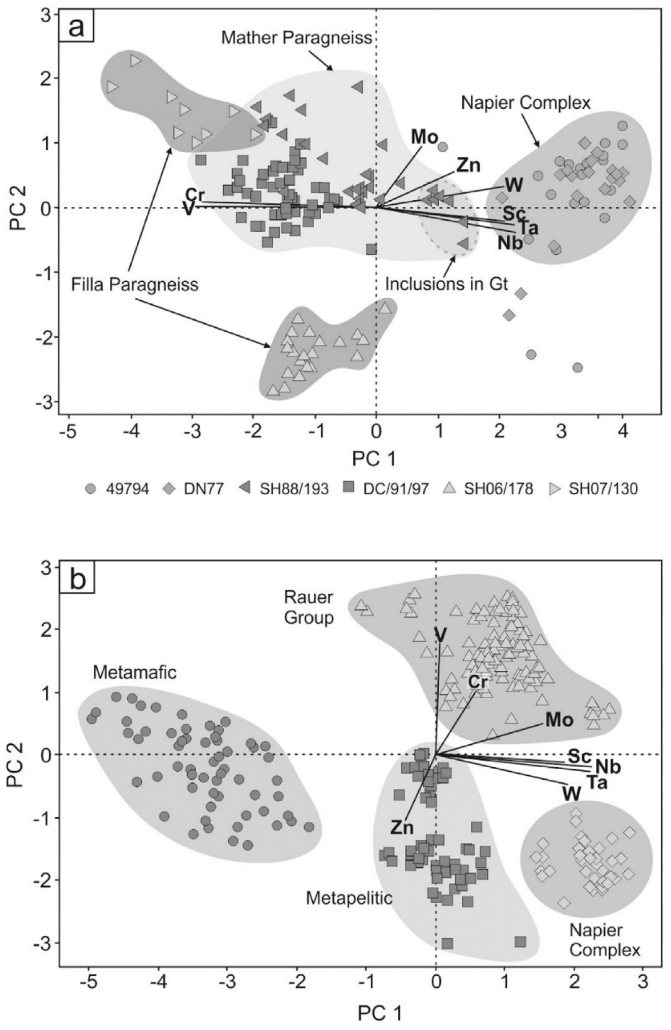

Fig. 3. PCA score and loading plots comparing (a) rutile trace element chemistry within each of the studied samples and (b) rutile trace element chemistry within Archean and Proterozoic UHT granulites compared to modern metamafic and metapelitic sediments. Metapelitic data comprises analyses of rutile from Syros, Greece and the Sesia Zone, Western Alps (taken from Hart et al., 2016), with analyses of metamafic rutile from the Monviso, Western Alps (unpublished data).

Material 2). Whilst rutiles from the Rauer Group samples do contain relatively high concentrations of Nb, Mo, Ta and W, they contain significantly higher concentrations of V and Cr. Rutiles from the Mather Paragneiss have the highest concentrations of Cr with 570–4340 ppm and generally plot in the top left quadrant. In sample SH88/193, rutile inclusions within a large garnet porphyroblast have significantly higher concentrations of Sc, Nb and W and lower V and Mo in comparison to matrix rutile and plot positively onto PC1 (Fig. 3a; Supplementary Material 2).

Rutiles from the Filla Paragneiss have the highest concentrations of V but contain less Cr and W than those from the Mather Paragneiss (Fig. 3a). Rutiles from sample SH07/130 plot in the top left quadrant as they contain the highest V concentrations of >6650 ppm, but the least amount of Nb, Ta and W out of all analysed samples. Rutiles from sample SH06/178 plot in the bottom left quadrant as they contain the most Nb but are less enriched in V and Cr in comparison to the other Rauer Group samples. Rutiles in sample SH06/178 also contain the least Mo (Fig. 3a; Supplementary Material 2).

As well as comparing trace element chemistry between the studied samples, PCA has also been utilised to determine if there are distinct differences between rutile formed under UHT and HP-LT conditions, which could have important implications for sediment provenance analysis. The scores and loadings plot in Fig. 3b shows that rutiles derived from UHT granulites are significantly enriched in V, Cr, Mo, Sc, Nb, Ta and W in comparison to rutile derived from HP-LT metapelitic and metamafic rocks. Rutiles derived from HP-LT metapelitic rocks contain slightly more Cr, Mo, Sc, Nb, Ta, W than HP-LT metamafic rutile, but less than rutiles from UHT granulites. Rutiles from HP-LT metamafic rocks contain the lowest concentrations of trace elements but have higher concentrations of V compared to rutiles derived from metapelitic rocks. The loadings show that Nb and V explain the most variance between samples, followed by Ta, Mo, Cr and W.

5.2. Zirconium concentrations in rutile

Rutile within samples DN77 and 49794 from the Archean Napier Complex are generally characterized by low Zr concentrations (Fig. 4; Supplementary Material 2). There is a pronounced cluster at ~700 ppm where approximately 93% of the analyses display low zirconium concentrations which correspond to temperatures 200 °C lower than expected for rocks which have undergone UHT metamorphism (>900 °C). Low Zr values are obtained for rutile that contains zircon inclusions or occurs close to or in contact with matrix zircon. Similar observations for rutile from comparable samples within the Napier Complex have been made by Harley (2008, 2016), as well as for rutile from granulites in the Ivrea-Verbano Zone (Luvizotto and Zack, 2009). Significantly higher Zr concentrations are recorded in a small number of rutile inclusions that occur primarily within orthopyroxene. Zirconium concentration in these rutiles ranges from 5480 ppm to 7910 ppm (Fig. 4).

In comparison, rutiles from the Rauer Group paragneisses are characterized by a remarkably large spread in Zr concentrations with multimodal distributions (Fig. 4). In the Mather Paragneiss, rutile from samples SH88/193 and DC/91/97 record Zr concentrations which range from 1220 ppm up to 3620 ppm (Fig. 4; Supplementary Material 2). The Zr data shows multimodal distribution with the main peak occurring around ~3200 ppm, with a smaller secondary peak visible in DC/91/97 at ~2500 ppm and lower concentrations ranging from 1300 to 1900 ppm.

Data obtained for rutiles from the Filla Paragneiss have a comparable multimodal distribution to the Mather Paragneiss (Fig. 4). Rutiles from sample SH06/178 cluster around ~3500 ppm, with a range of lower concentrations between 1400 and 2200 ppm. The peak at 3500 ppm is not visible in sample SH07/130, with most Zr concentrations ranging between 1500 ppm and 3500 ppm.

6. Mineral inclusions and intergrowths in rutile

Rutiles from each of the studied samples were investigated for inclusions and intergrowths that may aid in the interpretation of the trace element data. In the Napier Complex samples (DN77and 49794), rutile is found to contain numerous inclusions/intergrowths of aluminium silicate (Al_2SiO_5), with rare inclusions of quartz, corundum and mica (Fig. 5). Raman spectroscopy has identified the aluminium silicate in both samples as being kyanite, the high pressure, low temperature polymorph (Fig. 6). Kyanite occurs as acicular needles within rutile, often with multiple needles per grain (Fig. 5b–e). Intergrowths of orthopyroxene are common and in some rutiles are cross-cut by kyanite (Fig. 5b). Rare inclusions of corundum and mica are also found within rutiles from the Napier Complex (Fig. 5), and like kyanite, are not present within the matrix. The texture and morphology of corundum inclusions are not consistent with exsolution lamellae, and along with the rare mica inclusions, is interpreted to be part of the prograde assemblage. In the Rauer group, rutiles within the Mather Paragneiss samples (SH88/193 and DC/91/97) are largely free of inclusions and intergrowths, however some rutiles have intergrown with acicular sillimanite, with rare inclusions of quartz additionally found in sample SH88/193 (Fig. 5). No inclusions or intergrowths were observed in rutile from the Filla Paragneiss samples (SH07/130 and SH06/178).

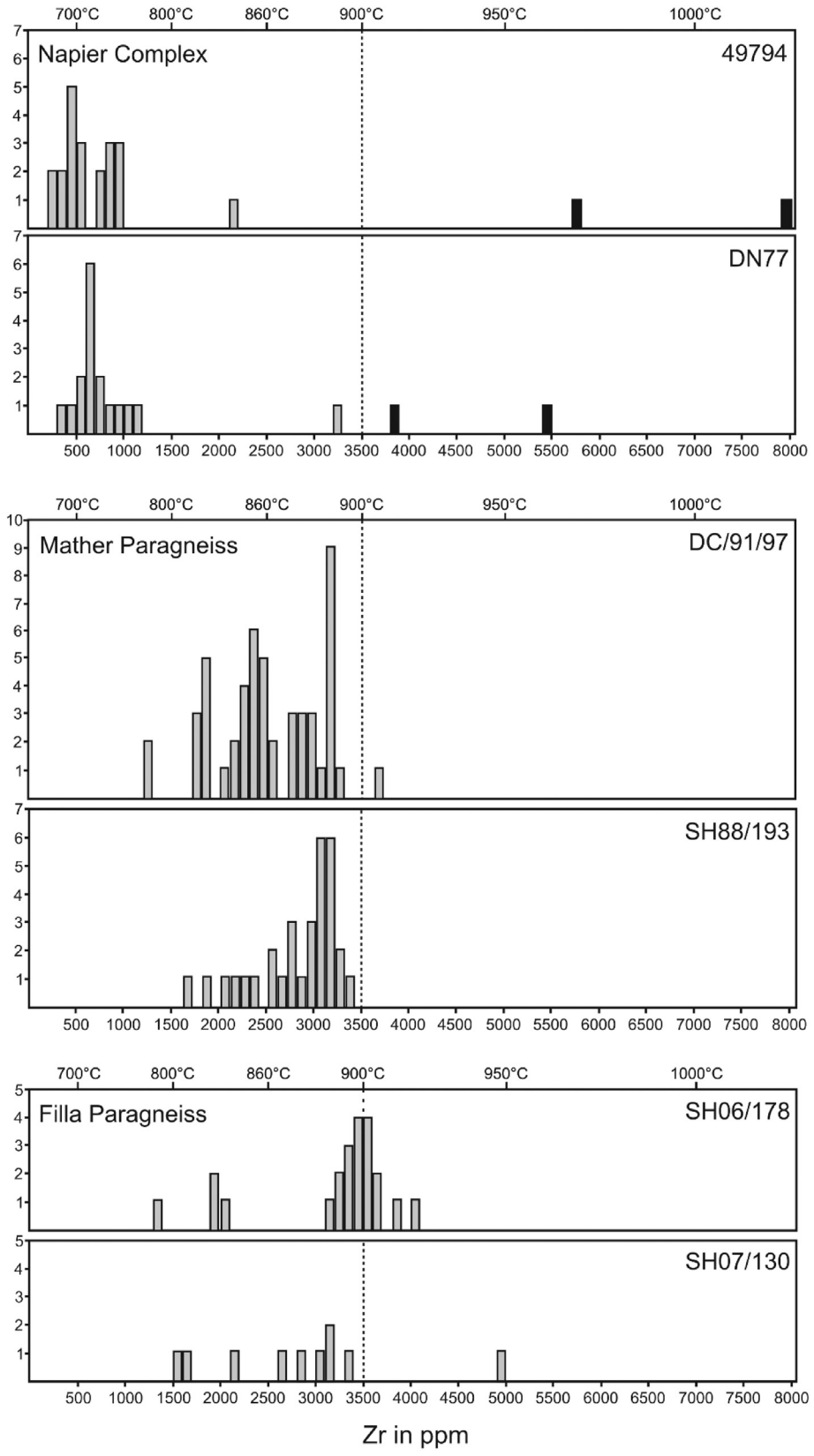

Fig. 4. Histograms showing the range of Zr concentrations in rutiles from (a) the Napier Complex, and the Mather (b) and Filla (c) paragneisses in the Rauer Group. Black boxes represent the Zr concentrations of rutile inclusions within orthopyroxene.

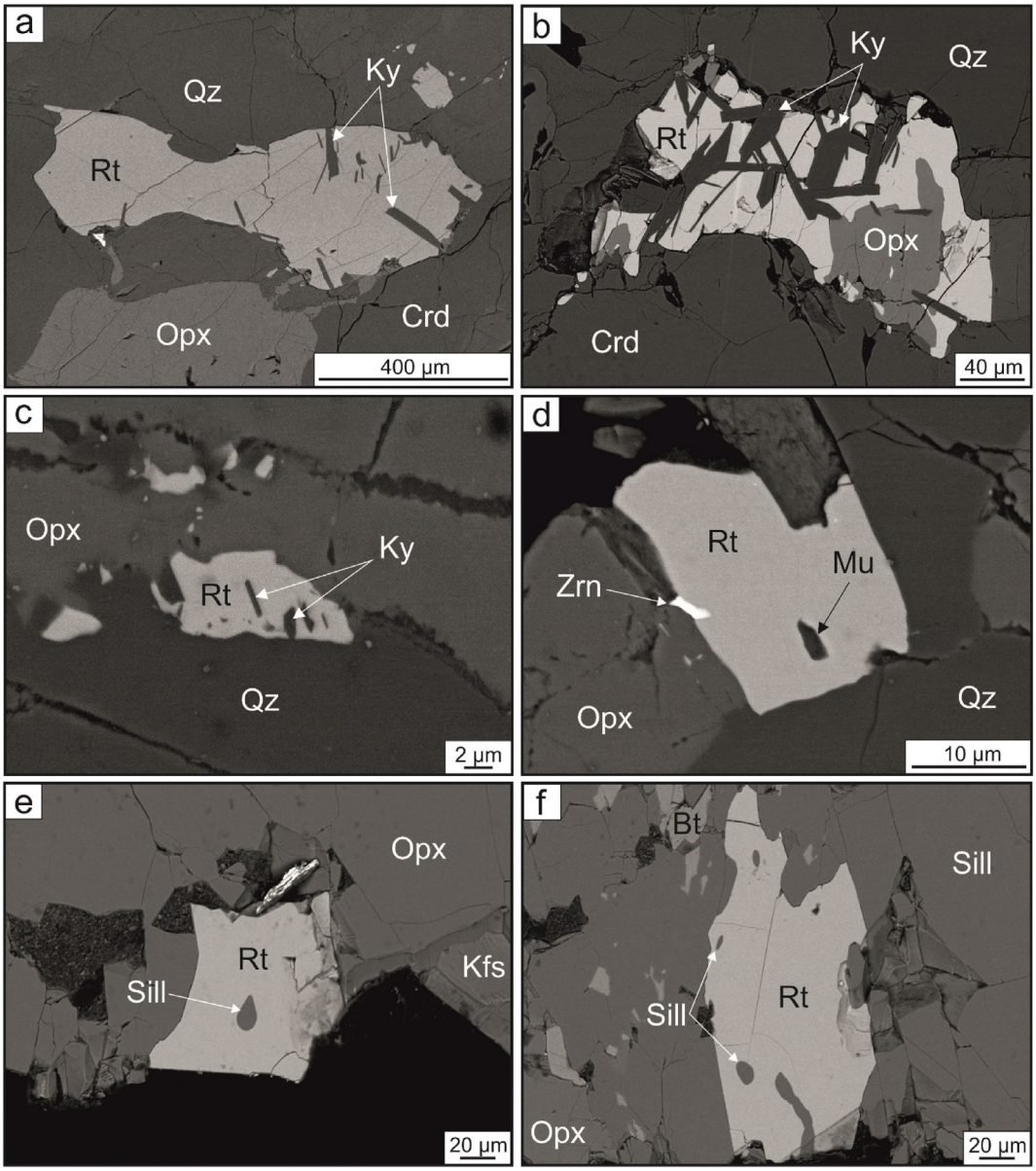

Fig. 5. BSE images showing inclusions/intergrowths in rutile from samples (a–b) DN77 and (c–d) 49794 (Napier Complex) and (e–f) sample DC/91/97 (Rauer Group).

7. Discussion

7.1. Trace element discrimination

Trace element concentrations in rutile can often be used to distinguish between source rock lithologies and locate potential sources of rutile in sediment provenance studies. However, the application of trace element discrimination, such as the Nb/Cr discrimination diagram, to rutile from Archean and early Proterozoic UHT terranes often result in analyses being misleadingly classified (e.g. Meyer et al., 2011; Kooijman et al., 2012).

To investigate this, PCA has been utilised to objectively identify which trace elements explain the most variance between rutile derived from UHT terranes and HP-LT metapelitic and metamafic rocks (Fig. 3b). However, as PCA plots are unsuitable for general discrimination (due to each dataset responding differently), the relative proportions of three elements identified by PCA to have the most variance have been used to create a ternary diagram.

Fig. 7 is a Nb-V-Cr ternary diagram comparing rutile from UHT terranes and HP-LT metapelitic and metamafic rocks. Nb, V and Cr were chosen as they account for the most variance and are routinely analysed rutile trace elements. Chromium was multiplied by 2 to improve the spread of the data.

The diagram shows that rutiles from HP-LT metamafic sources have high proportions of V, whereas low-temperature metapelitic rutile have higher proportions of Nb. Rutiles from the Napier Complex have the highest proportion of Nb, and plot close to low-temperature metapelitic rutile, unlike rutiles from the Mather and Filla paragneisses (Rauer Group) and other UHT granulite terranes which plot between low-temperature metapelitic and metamafic rutile in terms of V and Nb but differ in Cr concentration. UHT granulites derived from younger Mesoproterozoic and Neoproterozoic sources such as the Filla paragneiss and the Ivrea-Verbano Zone UHT granulites (e.g. Luvizotto and Zack, 2009) have lower concentrations of Cr compared to rutiles from the Mather paragneiss and Archean Pikwitonei Granulite Domain (Kooijman et al., 2012) which are significantly enriched in Cr (Fig. 9; Supplementary Material 2). This suggests that in comparison to modern sediments, the hinterland from which Archean and Proterozoic UHT metapelites are derived, may comprise ophiolitic or greenstone rocks with an abundance of Cr-rich minerals such as spinel.

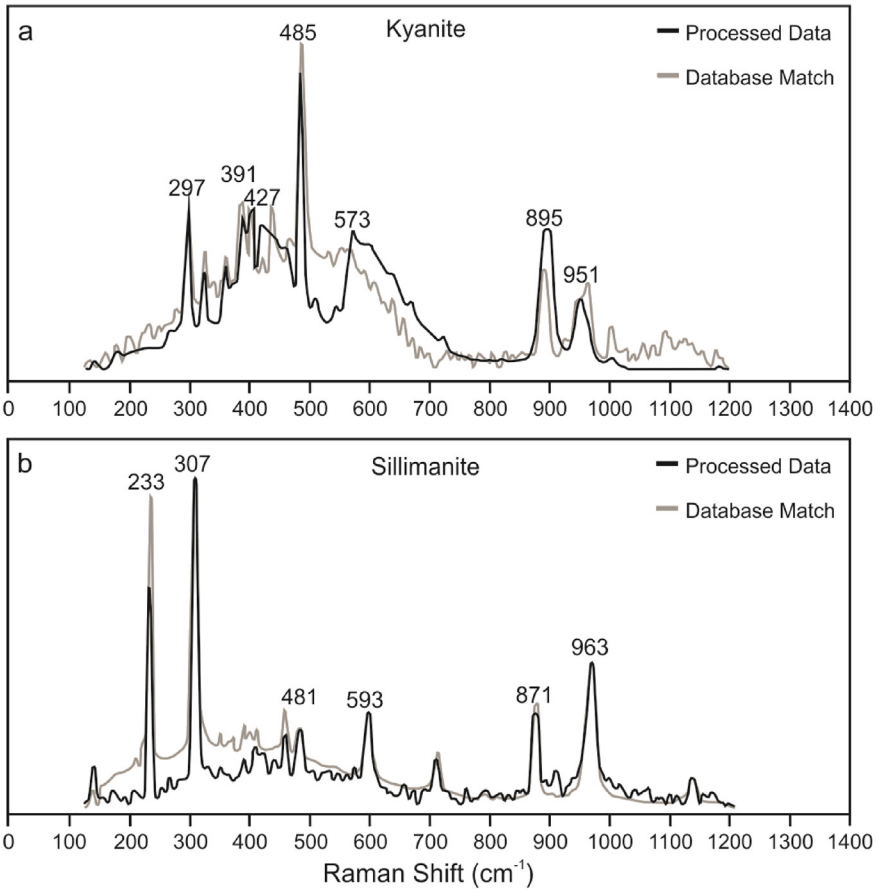

Fig. 6. Representative Raman spectra showing (a) kyanite inclusions found within rutile from the Napier Complex and (b) sillimanite found in the Mather Paragneiss, Rauer Group.

7.2. Zr-in-rutile geothermometry

The application of the Zr-in-rutile geothermometer to granulites that contain the assemblage rutile-quartz-zircon has the potential to recover evidence of UHT metamorphism. However, the interpretation of Zr data in granulite-facies rutile presents a challenge in terms of determining temperatures as rutile is often variably affected by post-peak processes (e.g. Taylor-Jones and Powell, 2015). For the purpose of this study, the calibration of Tomkins et al. (2007) has been used to calculate temperatures using maximum pressures of 11 kbar given in the

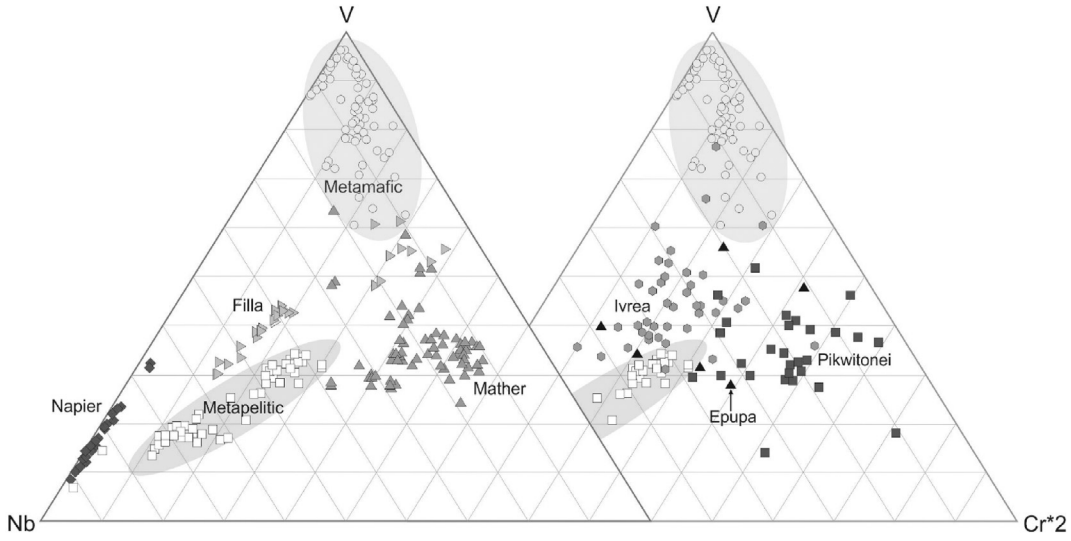

Fig. 7. Ternary diagram comparing the relative proportions of Nb, V and Cr in rutiles derived from Archean and Proterozoic UHT granulites to HP-LT metamafic and metapelitic rocks. Metapelitic data comprises analyses of rutile from the Sesia Zone, Western Alps (taken from Hart et al., 2016), with analyses of metamafic rutile from Syros, Greece (Hart et al., 2016) and the Monviso metaophiolite, Western Alps (unpublished data). Literature data taken from Luvizotto and Zack, 2009 (Ivrea Zone, Western Alps); Meyer et al., 2011 (Epupa Complex, NW Namibia) and Kooijman et al., 2012 (Pikwitonei Granulite Domain, Canada). Note that Cr was multiplied by 2 to improve the spread of the data.

literature for both the Napier Complex (e.g. Harley and Henson, 1990; Harley, 1998a; Shimizu et al., 2013) and Rauer Group (e.g. Harley, 1998b).

In the Archean Napier Complex, matrix rutiles have Zr concentrations of 230–2150 ppm (Fig. 4), corresponding to temperatures of 640–850 ± 30 °C at 11 kbar. These estimates are <200 °C lower than those needed for UHT metamorphism (>900 °C; Harley, 2008), and are below the temperatures required for the stability of sapphirine + quartz observed in the matrix. This is comparable to observations made in previous studies that rutiles in the Napier Complex record cooling temperatures of 660–740 °C (Harley, 2008, 2016). Recent studies have shown that rutile only has the capacity to retain peak UHT Zr concentrations if it is in chemical isolation from zircon (Luvizotto and Zack, 2009; Jiao et al., 2011; Kooijman et al., 2012; Ewing et al., 2013; Taylor-Jones and Powell, 2015; Pape et al., 2016). Rutiles which are closely associated with Zr-bearing phases, occurring either as small rounded inclusions, thin lamellae/acicular zircon exsolutions within rutile or as crystals which form adjacent to and around the rims of rutile (Fig. 8), exhibit the lowest Zr concentrations. Chemical communication between rutile and zircon during cooling results in the diffusion of Zr within and out of rutile down to the closure temperature of Zr in rutile in slowly-cooled rocks as determined by Cherniak et al. (2007).

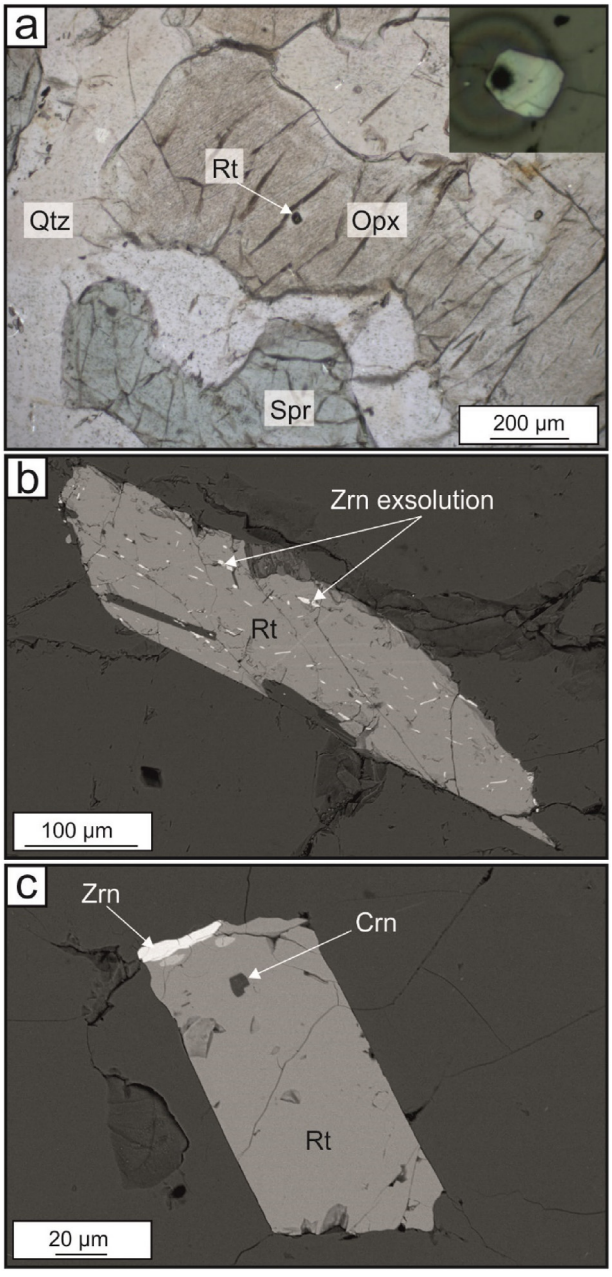

Fig. 8. Images showing (a) high Zr rutile inclusions within orthopyroxene, (b) rutile with zircon exsolution and (c) rutile in direct contact with zircon.

Unlike previous studies which have not recovered ultrahigh-temperatures directly from rutiles from the Napier Complex (Harley, 2008, 2016), several rutile grains which preserve higher Zr concentrations have been identified as part of this study (Figs. 4 and 8). These rutiles are found as inclusions primarily within orthopyroxene and retain Zr concentrations which are consistent with UHT conditions, unlike matrix rutile which record post-peak temperature conditions (Fig. 4). It has previously been suggested that under UHT conditions, host minerals with low Zr-diffusivity (e.g. garnet or pyroxene) can shield rutile inclusions from re-equilibration during post-peak processes (e.g. Zack et al., 2004b; Kooijman et al., 2012; Pauly et al., 2016). Zr concentrations of rutile inclusions range from 5480 to 7910 ppm, corresponding to temperatures of 950–1000 ± 30 °C. This supports peak temperatures of <1149 °C recently calculated for similar rocks within the Napier Complex by reintegrating zircon exsolution lamaellae to obtain the Zr concentrations of the host rutile prior to exsolution (Mitchell and Harley, 2017).

Rutiles from the Rauer Group paragneisses have a large spread in Zr concentrations (Fig. 4). A large spread in Zr concentrations appears to be unique to rutile formed under UHT metamorphic conditions (Luvizotto and Zack, 2009; Jiao et al., 2011; Meyer et al., 2011; Kooijman et al., 2012; Harley, 2016). This may be due to the effect of post-peak processes which mobilize certain elements such as Zr resulting in the variable resetting of Zr concentrations in rutile (Jiao et al., 2011). Calculated temperatures between the lowest and highest Zr concentrations are therefore meaningless as the rutile in these samples have undergone variable resetting as a result of cooling with decompression from 1050 °C and 1.2 GPa through to 900 °C and 0.7–0.8 GPa (Harley, 1998b). In order to constrain near-peak temperatures, only values between the 90th percentile and the maximum have been considered as the grains with the highest Zr concentrations should be the least affected by resetting (Luvizotto and Zack, 2009). On this basis, rutiles from the Mather Paragneiss with Zr concentrations ranging between 3170 and 3610 ppm record an upper temperature range of 880–900 ± 30 °C at 0.9 GPa (Fig. 4). A similar spread in rutile Zr concentrations has been described in the Mather Paragneiss (Harley, 2016) but temperature estimates obtained were lower than those obtained in this study and did not record UHT temperatures. In this study, the maximum temperatures obtained are >930 °C (including the 30 °C error) which are only 20 °C lower than previous estimates (950–1030 °C; Harley and Fitzsimons, 1991; Harley, 1998b, 2004; Kelsey et al., 2004, 2005; Harley, 2008) and this is consistent with UHT metamorphism. Temperatures calculated for the Filla Paragneiss on the other hand are slightly higher than those obtained for the Mather Paragneiss, with Zr concentrations between 3850 and 4910 ppm giving an upper estimate between 910 and 950 ± 30 °C at 10 kbar (Fig. 4). The presence of sillimanite and the shared metamorphic history with the Mather Paragneiss has led to previous studies suggesting minimum temperatures of 840 ± 40 °C (Harley and Fitzsimons, 1991; Harley and Buick, 1992).

7.3. Preservation of prograde kyanite in UHT rutile

Although the prograde history of UHT rocks is often poorly preserved owing to rapid diffusion and reaction rates (Hollis et al., 2006), it has recently been demonstrated that rutile is an excellent container for the preservation of mineral inclusions and is capable of preserving prograde phases in rocks that otherwise have no trace of the prograde assemblage within the matrix (Hart et al., 2016). Rutile is known to be resistant to fluid infiltration (Zack et al., 2004b; Triebold et al., 2007), and like garnet and zircon has a low compressibility meaning that it has a remarkable confining strength which exerts an overpressure on inclusions during exhumation (Hart et al., 2016). In addition,

observations have shown that inherent anisotropies, such as rutile's distinct [110] cleavage and a tendency for twinning, do not appear to be major weaknesses or pathways for preferential retrogression and do not inhibit the preservation of mineral inclusions.

The majority of inclusion/intergrowth-bearing rutiles are found within samples from the Napier Complex, and largely comprise kyanite, a phase which is not present within the matrix. As the occurrence of kyanite in the Napier Complex samples is restricted to within rutile, kyanite is interpreted to be a prograde phase. The abundance of kyanite indicates metastability and phase control by local chemical potential gradients and topotaxial considerations, which further supports this interpretation. Whilst inclusions of prograde phases such as kyanite and staurolite have been found within garnet and plagioclase in the neighbouring Lützow-Holm Complex, Antarctica (Shimpo et al., 2006), the preservation of petrological evidence from the prograde path is uncommon among the UHT terranes of East Antarctica. The UHT *P-T* evolution of the Napier Complex has long been debated due to the lack of preserved prograde phases, with support for both clockwise and counter-clockwise paths (e.g. Ellis, 1987; Motoyoshi and Hensen, 1989; Harley, 1989, 1991; Harley and Black, 1997; Tsunogae et al., 2002; Hokada et al., 2008). This important new discovery provides the first direct evidence that the Napier Complex experienced a clockwise *P-T* path (Fig. 9), proceeding through 900 °C and 1.0–1.1 GPa. The preservation of rutiles with Zr concentrations corresponding to UHT conditions, indicates a thermal excursion to over 1000 °C into the Spr + Grt + Sil + Qz field (Spl,Crd,Opx) in FMAS, with near-peak decompression into the Spr + Opx + Qtz field for magnesian rocks, before near-isobaric cooling to 700 °C and 0.7 GPa.

8. Conclusions

This study demonstrates that although trace element behaviour in rutile can be difficult to interpret in UHT granulites, reliable temperature estimates can be obtained by applying the Zr-in-rutile thermometer to rutiles which are armoured within other phases (e.g. orthopyroxene), with additional constraints from intergrowths of prograde kyanite within rutile. The main conclusions, and aspects requiring caution and further study, are summarised below.

- Metapelitic rutile from Archean and Proterozoic UHT terranes are significantly enriched in trace elements in comparison to those from modern metasediments.
- Rutile grains which occur in contact with or adjacent to zircon record temperatures lower than expected. Post-UHT fluid-rock interaction results in significant zircon recrystallization and variable resetting of Zr concentrations in rutile.
- Rutile grains occurring as inclusions within other phases have been shielded from post-peak diffusional resetting and record UHT conditions.
- The large spread in Zr concentrations obtained for rutiles from the Rauer Group is related to post-peak diffusional resetting associated with decompression with cooling and/or the presence of fluid.
- UHT rutiles preserve mineral inclusions/intergrowths of prograde and peak phases, with prograde kyanite providing the first direct evidence that the Napier Complex experienced a typical clockwise *P-T* evolution.

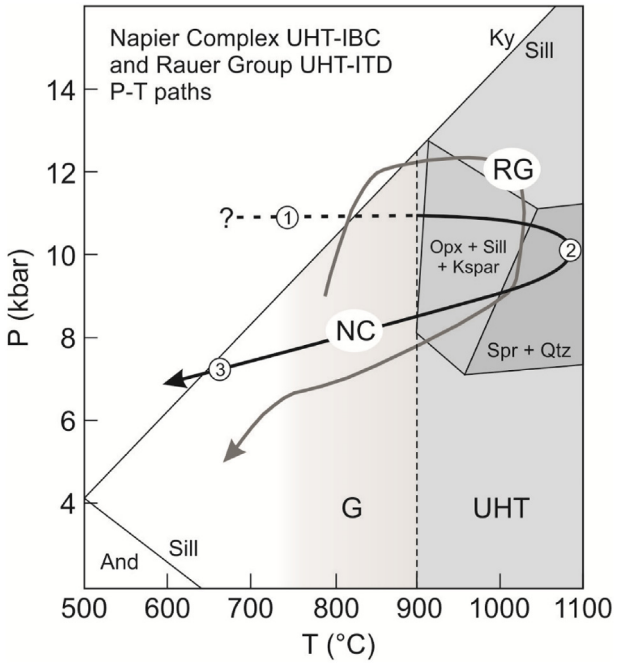

Fig. 9. *P-T* diagram showing the clockwise UHT-IBC path of the Napier Complex in comparison to the UHT-ITD path of the Rauer Group paragneisses (modified after Harley, 2016). It is inferred from the occurrence of prograde kyanite, and Zr-in-rutile temperatures, that the *P-T* path of the Napier Complex metapelites (1) traversed up through 900 °C and 1.0–1.1 GPa, taking (2) a thermal excursion up over 1000 °C, with near-peak decompression, before (3) near-isobaric cooling down to 700 °C and 0.7 GPa.

Supplementary data to this article can be found online at https://doi.org/10.1016/j.gr.2018.02.021.

Acknowledgements

We would firstly like to thank the editor and the two anonymous reviewers for their constructive comments which have helped to improve this manuscript. Stuart Kearns at the University of Bristol is thanked for his assistance using the electron microprobe, as is Bruce Alexander at the University of Greenwich for assistance with the Raman microscope. This project was funded by NERC grant NE/I025573 awarded to PI Storey, including a NERC studentship for Emma Hart. Samples used in this study were collected by S.L. Harley with the support of the Australian National Antarctic Research Expeditions (ANARE) 1979–80, 1987–88, 1991–92 and 2006–07, logistics funding under Australian Antarctic Science project grants 263, 497 and 2690 to Harley, and fieldwork funding under NERC grant NE/B504157/1 (2004–2007) awarded to Harley.

References

Carson, C.J., Ague, J.J., Coath, C.D., 2002. U-Pb geochronology from Tonagh Island, East Antarctica: implications for the timing of ultra-high temperature metamorphism of the Napier Complex. Precambrian Research 116, 237–263.
Cherniak, D.J., Manchester, J., Watson, E.B., 2007. Zr and Hf diffusion in rutile. Earth and Planetary Science Letters 261, 267–279.
Dallwitz, W.B., 1968. Chemical composition and genesis of clinoenstatite-bearing volcanic rocks from Cape Vogel, papua: a discussion. Proceedings 23rd International Geological Congress, 2, pp. 229–242.
Ellis, D.J., 1987. Origin and evolution of granulites in normal and thickened crusts. Geology 15, 167–170.
Ewing, T.A., Hermann, J., Rubatto, D., 2013. The robustness of the Zr-in-rutile and Ti-in-zircon thermometers during high-temperature metamorphism (Ivrea-Verbano Zone, northern Italy). Contributions to Mineralogy and Petrology 165, 757–779.
Guillong, M., Meier, D.L., Allan, M.M., Heinrich, C.A., Yardley, B.W.D., 2008. Sills: a matlab-based programme for the reduction of laser ablation ICP-MS data of homogenous materials and inclusions. Mineralogical Association of Canada, 40, pp. 328–333.
Harley, S.L., 1989. The origins of granulites: a metamorphic perspective. Geological Magazine 126, 215–247.
Harley, S.L., 1991. The crustal evolution of some East Antarctic granulites. In: Thomson, M.R.A., Crame, J.A., Thomson, J.W. (Eds.), Geological Evolution of Antarctica. Cambridge University Press, Cambridge, pp. 7–12.
Harley, S.L., 1998a. On the occurrence and characterization of ultrahigh-temperature crustal metamorphism. Geological Society, London, Special Publications 138, 81–107.
Harley, S.L., 1998b. Ultrahigh temperature granulite metamorphism (1050 °C, 12 kbar) and decompression in garnet (Mg70)-orthopyroxene-sillimanite gneisses from the Rauer Group, East Antarctica. Journal of Metamorphic Geology 16, 541–562.
Harley, S.L., 2004. Extending our understanding of ultrahigh temperature crustal metamorphism. Journal of Mineralogical and Petrological Sciences 99, 140–158.S.
Harley, S.L., 2008. Refining the *P-T* records of UHT crustal metamorphism. Journal of Metamorphic Geology 26, 125–154.

Harley, S.L., 2016. A matter of time: the importance of the duration of UHT metamorphism. Journal of Mineralogical and Petrological Sciences 111, 50–72.
Harley, S.L., Black, L.P., 1997. A revised Archean chronology for the Napier Complex, Enderby Land, from SHRIMP ion-microprobe studies. Antarctic Science 9, 74–91.
Harley, S.L., Buick, I.S., 1992. Wollastonite-scapolite assemblages as indicators of granulite pressure-temperature-fluid histories: the Rauer Group, East Antarctica. Journal of Petrology 33, 693–728.
Harley, S.L., Fitzsimons, I.C.W., 1991. Pressure-temperature evolutions of metapelitic granulites in a polymetamorphic terrane: the Rauer Group, East Antarctica. Journal of Metamorphic Geology 9, 231–243.
Harley, S.L., Henson, B.J., 1990. Archaean and Proterozoic high-grade terranes of East Antarctica (40DE400E): a case study of the diversity in granulite facies metamorphism. In: Ashworth, J.R., Brown, M. (Eds.), High Temperature Metamorphism and Crustal Anatexis. Unwin Hyman, London, pp. 320–370.
Harley, S.L., Motoyoshi, Y., 2000. Al zoning in orthopyroxene in a sapphirine quartzite: evidence for >1120 °C UHT metamorphism in the Napier Complex, Antarctica, and implications for the entropy of sapphirine. Contributions to Mineralogy and Petrology 138, 293–307.
Hart, E., Storey, C., Bruand, E., Schertl, H.-P., Alexander, B.D., 2016. Mineral inclusions in rutile: a novel recorder of HP-UHP metamorphism. Earth and Planetary Science Letters 446, 137–148.
Hokada, T., Misawa, K., Shiraishi, K., Suzuki, S., 2003. Mid to late Archean (3.3–2.5 Ga) tonalitic crustal formation and high-grade metamorphism at Mt. Riiser-Larsen, Napier Complex, East Antarctica. Precambrian Research 127, 215–228.
Hokada, T., Misawa, K., Yokoyama, K., Shiraishi, K., Yamaguchi, A., 2004. SHRIMP and electron microprobe chronology of UHT metamorphism in the Napier Complex, East Antarctica: implications for zircon growth at >1000 °C. Contributions to Mineralogy and Petrology 147, 1–20.
Hokada, T., Motoyoshi, Y., Suzuki, S., Ishikawa, M., Ishizuka, H., 2008. Geodynamic evolution of Mt. Riiser Larsen, Napier Complex, East Antarctica, with reference to the UHT mineral associations and their reaction relations. Geological Society, London, Special Publications 308, 253–282.
Hokada, T., Harley, S.L., Dunkley, D.J., Kelly, N.M., Yokoyama, K., 2016. Peak and post-peak development of UHT metamorphism at Mather Peninsula, Rauer Islands: zircon and monazite U-Th-Pb and REE chemistry constraints. Journal of Mineralogical and Petrological Sciences 111, 89–103.
Hollis, J.A., Harley, S.L., White, R.W., Clarke, G.L., 2006. Preservation of evidence for prograde metamorphism in ultrahigh-temperature, high-pressure kyanite-bearing granulites, South Harris, Scotland. Journal of Metamorphic Geology 24, 263–279.
Horie, K., Hokada, T., Hiroi, Y., Motoyoshi, Y., Shiraishi, K., 2012. Contrasting Archean crustal records in western part of the Napier Complex, East Antarctica: new constraints from SHRIMP geochronology. Gondwana Research 21, 829–837.
Jiao, S., Guo, J., Mao, Q., Zhao, R., 2011. Application of Zr-in-rutile thermometry: a case study from ultrahigh-temperature granulites of the Khondalite belt, North China Craton. Contributions to Mineralogy and Petrology 162, 379–393.
Kelly, N.M., Harley, S.L., 2005. An integrated microtextural and chemical approach to zircon geochronology: refining the Archean history of the Napier Complex, East Antarctica. Contributions to Mineralogy and Petrology 149, 57–84.
Kelsey, D.E., Hand, M., 2015. On ultrahigh temperature crustal metamorphism: phase equilibria, trace element thermometry, bulk composition, heat sources, timescales and tectonic settings. Geoscience Frontiers 6, 311–356.
Kelsey, D.E., Powell, R., Wilson, C.J.L., Steele, D.A., 2003a. (Th + U) − Pb monazite ages from Al-Mg-rich metapelites, Rauer Group, east Antarctica. Contributions to Mineralogy and Petrology 146, 236–340.
Kelsey, D.E., White, R.W., Powell, R., Wilson, C.J.L., Quinn, C.D., 2003b. New constraints on metamorphism in the Rauer Group, Prydz Bay, East Antarctica. Journal of Metamorphic Geology 21, 739–759.
Kelsey, D.E., White, R.W., Holland, T.J.B., Powell, R., 2004. Calculated phase equilibria in K_2O–MgO–FeO–Al_2O_3–SiO_2–H_2O for sapphirine–quartz-bearing mineral assemblages. Journal of Metamorphic Geology 22, 559–578.
Kelsey, D.E., White, R.W., Powell, R., 2005. Calculated phase equilibria in K_2O–MgO–FeO–Al_2O_3–SiO_2–H_2O for silica-undersaturated sapphirine-bearing mineral assemblages. Journal of Metamorphic Geology 23, 217–239.
Kelsey, D.E., Hand, M., Clarke, C., Wilson, C.J.L., 2007. On the application of in situ monazite chemical geochronology to constraining P-T-*t* histories in high temperature (>850 °C) polymetamorphic granulites from Prydz Bay, East Antartica. Journal of the Geological Society, London 164, 667–683.
Kelsey, D.E., Wade, B.P., Collins, A.S., Hand, M., Sealing, C.R., Netting, A., 2008. Discovery of a Neoproterozoic basin in the Prydz belt in East Antarctica and its implications for Gondwana assembly and ultrahigh temperature metamorphism. Precambrian Research 161, 335–388.
Kooijman, E., Smit, M.A., Mezger, K., Berndt, J., 2012. Trace element systematics in granulite facies rutile: implication for Zr geothermometry and provenance studies. Journal of Metamorphic Geology 30, 397–412.
Laetsch, T., Downs, R., 2006. Software for identification and refinement of cell parameters from powder diffraction data of minerals using the RRUFF project and American mineralogist crystal structure databases. Abstracts From the 19th General Meeting of the International Mineralogical Association, Kobe, Japan, 23–28 July 2006.
Lafuente, B., Downs, R.T., Yang, H., Stone, N., 2015. The power of databases: the RRUFF project. In: Armbruster, T., Danisi, R.M. (Eds.), Highlights in Mineralogical Crystallography. W. De Gruyter, Berlin, Germany, pp. 1–30.
Luvizotto, G.L., Zack, T., 2009. Nb and Zr behaviour in rutile during high-grade metamorphism and retrogression: an example from the Ivrea-Verbano Zone. Chemical Geology 261, 303–317.
Luvizotto, G.L., Zack, T., Meyer, H.P., Ludwig, T., Triebold, S., Kronz, A., Münker, C., Stockli, D.F., Prowatke, S., Klemme, S., Jacob, D.E., von Eynatten, H., 2009. Rutile crystals as potential trace element and isotope mineral standards for microanalysis. Chemical Geology 261, 346–369.
Meinhold, G., Anders, B., Kostopoulos, D., Reischmann, T., 2008. Rutile chemistry and thermometry as provenance indicator: an example from Chios Island, Greece. Sedimentary Geology 203, 98–111.
Meyer, M., John, T., Brandt, S., Klemd, R., 2011. Trace element composition of rutile and the application of Zr-in-rutile thermometry to UHT metamorphism (Epupa Complex, NW Namibia). Lithos 126, 388–401.
Mitchell, R.J., Harley, S.L., 2017. Zr-in-rutile resetting in aluminosilicate bearing ultra-high temperature granulites: refining the record of cooling and hydration in the Napier Complex, Antarctica. Lithos 272–273, 128–146.
Motoyoshi, Y., Hensen, B.J., 1989. Sapphirine–quartz–orthopyroxene symplectites after cordierite in the Archaean Napier Complex, Antarctica: evidence for a counterclockwise P–T path? European Journal of Mineralogy 1, 467–471.
Pape, J., Mezger, K., Robyr, M., 2016. A systematic evaluation of the Zr-in-rutile thermometer in ultra-high temperature (UHT) rocks. Contributions to Mineralogy and Petrology 171, 1–20.
Pauly, J., Marschall, H.R., Meyer, H.-P., Chatterjee, N., Monteleone, B., 2016. Prolonged Ediacaran–Cambrian metamorphic history and short-lived high-pressure granulite facies metamorphism in the H.U. Sverdrupfjella, Dronning Maud Land (East Antarctica): evidence for continental collision during Gondwana assembly. Journal of Petrology 57, 185–228.
Pearce, N.J.G., Perkins, W.T., Westgate, J.A., Gorton, M.P., Jackson, S.E., Neal, C.R., Chenery, S.P., 1997. A compilation of new and published major and trace element data for NIST SRM 610 and NIST SRM 612 glass reference materials. The Journal of Geostandards and Geoanalysis 21, 115–144.
Sheraton, J.W., Tingrey, R.J., Black, L.P., Offe, L.A., Ellis, D.J., 1987. Geology of an unusual Precambrian high-grade metamorphic terrane – Enderby land and western Kemp land, Antarctica. Bureau of Mineral Resources Bulletin 223, 51.
Shimizu, H., Tsunogae, T., Santosh, M., 2013. Petrology and phase equilibrium modelling of sapphirine + quartz assemblage from the Napier Complex, East Antarctica: diagnostic evidence for Neoarchean ultrahigh-temperature metamorphism. Geoscience Frontiers 4, 655–666.
Shimpo, M., Tsunogae, T., Santosh, M., 2006. First report of garnet–corundum rocks from southern India: implications for prograde high-pressure (eclogite-facies?) metamorphism. Earth and Planetary Science Letters 242, 111–129.
Taylor-Jones, K., Powell, R., 2015. Interpreting zirconium-in-rutile thermometric results. Journal of Metamorphic Geology 33, 115–122.
Tomkins, H.S., Powell, R., Ellis, D.J., 2007. The pressure dependence of the zirconium-in-rutile thermometer. Journal of Metamorphic Geology 25, 703–713.
Tong, L., Wilson, C.J.L., 2006. Tectonothermal evolution of the ultrahigh temperature metapelites in the Rauer Group, east Antarctica. Precambrian Research 149, 1–20.
Triebold, S., von Eynatten, H., Luvizotto, G.L., Zack, T., 2007. Deducing source rock lithology from detrital rutile geochemistry: an example from the Erzgebirge, Germany. Chemical Geology 244, 421–436.
Tsunogae, T., Santosh, M., Osanai, Y., Owada, M., Toyoshima, T., Hokada, T., 2002. Very high-density carbonic fluid inclusions in sapphirine-bearing granulites from Tonagh Island in the Archean Napier Complex, East Antarctica: implications for CO_2 infiltration during ultrahigh-temperature (T > 1,100 °C) metamorphism. Contributions to Mineralogy and Petrology 143, 279–299.
Watson, E.B., Wark, D.A., Thomas, J.B., 2006. Crystallization thermometers for zircon and rutile. Contributions to Mineralogy and Petrology 151, 413–433.
Zack, T., Moraes, R., Kronz, A., 2004a. Temperature dependence of Zr in rutile: empirical calibration of a rutile thermometer. Contributions to Mineralogy and Petrology 148, 471–488.
Zack, T., Eynatten, H.V., Kronz, A., 2004b. Rutile geochemistry and its potential use in quantitative provenance studies. Sedimentary Geology 171, 37–58.